TECHNICAL MEMORANDUM

105

The impact of the El Niño anomaly on the mean meridional circulation as simulated by a high resolution model

Guo xiong Wu and U. Cubasch

Research Department

August 1985

European Centre for Medium-Range Weather Forecasts
Europäisches Zentrum für mittelfristige Wettervorhersage
Centre européen pour les prévisions météorologiques à moyen

Abstract

High resolution experiments with the operational ECMWF model starting from observed data were used to test the impact of the 1982/83 El Nino sea surface temperature anomaly on the zonal mean circulation.

As suggested by Bjerknes (1966, 1969) the increased sea surface temperature amplifies the Hadley circulation. However, contrary to Bjerknes' hypothesis the subtropical jet does not increase significantly but moves towards the equator. It is speculated that the northward shift of the subtropical jet, which is common to a number of model simulations, is therefore caused by an underestimation of the Hadley circulation and/or its driving mechanism.

C O N T E N T S

1. INTRODUCTION

During recent years a number of papers have been published covering various aspects of the impact of sea surface temperatures on the atmospheric circulation. For a comprehensive review see Shukla and Wallace, 1983.

All these studies, however, do not make any attempt to diagnose the changes in the mean meridional transfers invoked by the altered SST, but rather limit themselves to side by side comparisons and/or statistical evaluations. This is somewhat surprising since Bjerknes (1966, 1969) in his observational study of the impact of the El Nino SST anomalies on the atmospheric circulation speculated that a warmer SST in the tropical ocean strengthens the Hadley circulation. Also he concluded from momentum balance considerations that the westerlies in the mid-latitudes have to increase. While Cubasch (1985) verified most of Bjerknes' hypothesis using a synoptic evaluation of model simulations, this investigation concentrates upon the influence of a SST anomaly on the mean meridional circulation and on the meridional transfer of heat and moisture. Even though the El Nino SST anomaly covers only a quarter of the globe, it appears to be large enough for its effects to be diagnosed in the zonal mean. The results described in this report provide information about the mean meridional circulation which may be of use to scientists dealing with two-dimensional models.

After a short description of the model and the data involved (Section 2), the zonal mean circulation (Section 3.1) and the meridional transfers (Section 3.2) will be discussed. This is followed by a consideration of the budgets of heat and moisture (Section 3.3).

$A_{k+\frac{1}{2}}$ (mb)	$B_{k+\frac{1}{2}}$
0	0
50	0
99	0.002
142	0.013
173	0.042
191	0.094
194	0.170
182	0.268
157	0.384
125	0.511
89	0.638
54	0.756
26	0.856
8	0.929
0	0.973
0	0.992
0	1

Vertical Coordinate Table (NL=16)

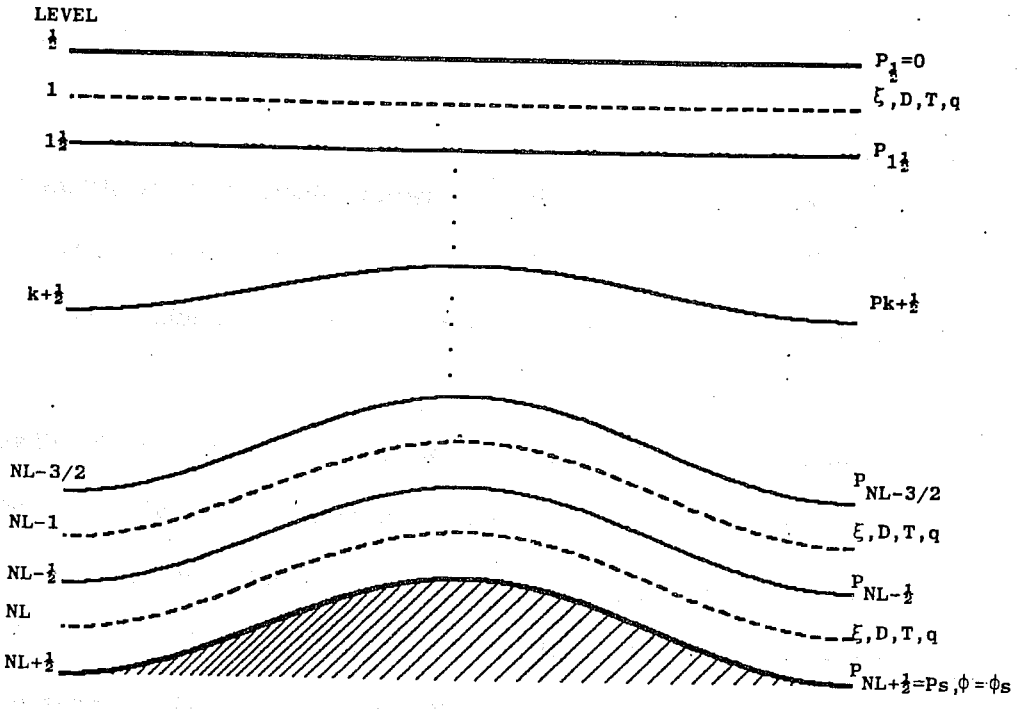

Disposition of variables in the vertical

Dependent variables	ξ,D,T,q,ln(ps)
Vertical coordinate	Hybrid, $P_{k+\frac{1}{2}}=A_{k+\frac{1}{2}}+B_{k+\frac{1}{2}}Ps$, details as above.
Vertical representation	Finite-difference, energy and angular-momentum conserving.
Horizontal representation	Spectral, with triangular truncation at wavenumber 63.
Horizontal grid	96x192 points on a quasi-regular ($\approx 1.875^{o}$) "Gaussian"grid.
Time integration	Leapfrog, semi-implicit (Δt=20 min), time filter (V=0.06).
Horizontal diffusion	Linear, fourth-order ($K=2\times10^{15} m^4 s^{-1}$).
Orography	Grid-scale average from high resolution data set, spectrally- fitted, "mean" orography.
Vertical boundary conditions	Kinematic.
Physical parameterisation	(i) Boundary eddy fluxes dependent on local roughness length and stability (Monin Obukov).
	(ii) Free-atmosphere turbulent fluxes dependent on mixing length and Richardson number.
	(iii) Kuo convection scheme.
	(iv) Interaction between radiation and model-generated clouds. Albedo dependent on model snow cover.
	(v) Large-scale condensation when grid-square saturated. Evaporation of precipitation.
	(vi) Computed land temperature, no diurnal cycle.
	(vii) Computed soil moisture and snow cover.
	(viii) Fixed, analysed sea-surface temperature.

Fig. 1. The ECMWF forecasting model.

2. THE EXPERIMENT

2.1 The model

The model used for all the experiments was the operational forecasting model (spring 1984) of the ECMWF (Louis, 1984). It has a horizontal resolution up to zonal wavenumber 63 and a vertical resolution of 16 level. For further details see Fig. 1.

The physical parameterisation is performed on a Gaussian grid, which has a resolution of 1.875°; it includes a full hydrological cycle. The radiation scheme includes the diurnal cycle and the angle of the sun according to the date. The surface boundary conditions (SST, soil-moisture, soil-wetness) are kept constant at their initial value. The orography used was the version referred to as "mean" orography, which was used operationally until March 1983.

2.2 The data

The initial condition for the simulations was the operational ECMWF analysis for 1 January 1983. The SST for the control experiment was the mean January climate (Alexander and Mobley, 1974). In the anomaly case the climatological SST has been changed in the Pacific region by the addition of the El Nino anomaly as observed during January 1983 (Fig. 2). This anomaly was made available by the CAC in Washington (Reynolds, 1983, pers. com.)

3. RESULTS

Both experiments were integrated for 40 days. In this study the mean fields taken from day 11 to day 40 are considered. The short integration time,

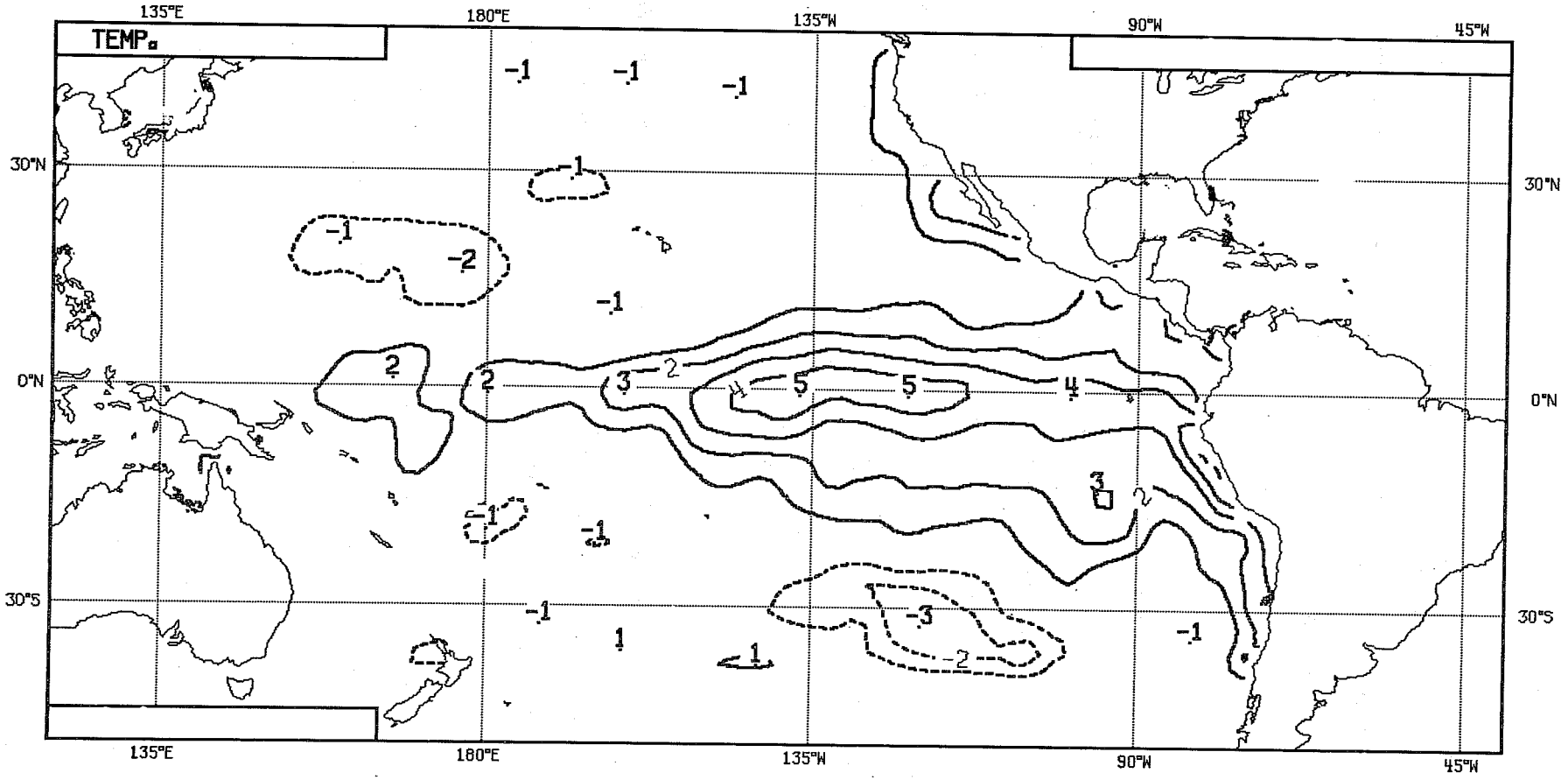

Fig. 2 The observed SST anomaly in the Pacific during January 1983 - Reynolds (1983). Units: ^{o}C.

which is too short to allow the model to reach its equilibrium (Cubasch, 1981), was chosen for economic reasons. However, comparisons with longer integrations (Cubasch, 1985) indicates that the predominant effects of the SST anomaly emerge during 40 day integrations.

3.1 Zonal mean quantities

Fig. 3 shows the temperature differences between the control and anomaly cases. During the integration the troposphere in the tropics is warmed by the El Nino with a maximum of more than 2K at 250mb, while the stratosphere has been cooled by a maximum of 1.4K at 150mb. In the mid-latitudes of the northern hemisphere the atmosphere is cooled by about 1K. Most strikingly the north polar region is warmed by about 6K in the lower troposphere and 3K in the stratosphere above 100mb. The tropospheric warming in the tropics and subtropics has a similar structure to that found in longer integrations (Cubasch, 1985). It is interesting to note the warming in the stratosphere which could also be found in the observations (Greb and Nanjokat, 1983), but could not be linked with the El Nino.

The experiments also show that the moisture content in the tropical areas appears to be increased by the SST anomaly, but decreased in the subtropics. Table 1 shows the vertical distribution of specific humidity at the equator for the two experiments and the difference between them. Clearly the El Nino SST anomaly causes an increase in the humidity.

The intensities of the tropical easterlies in the stratosphere and the westerly jets in the two hemispheres do not change substantially (Fig. 4). However, the mid-latitude jets extend more equatorwards, resulting in

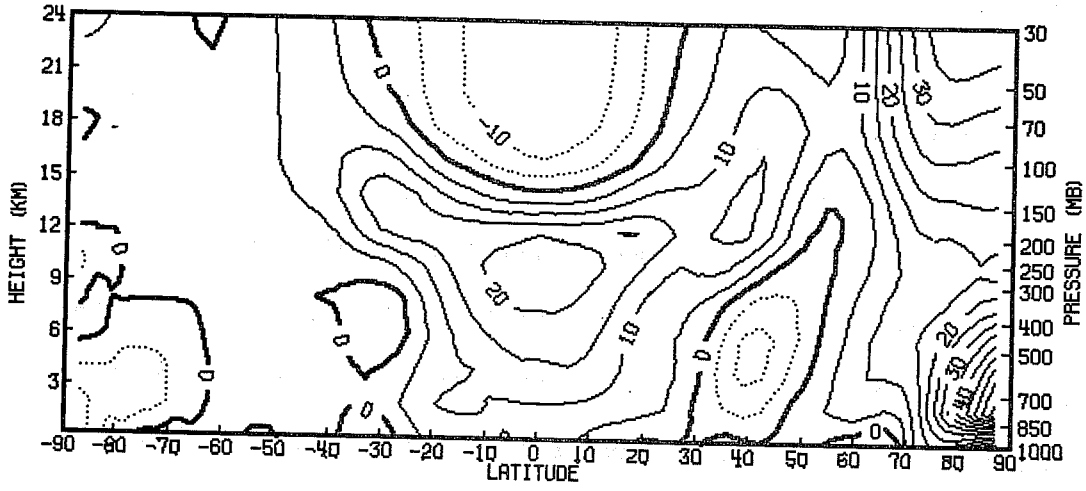

Fig. 3 The difference in the zonal mean temperature (El Nino-Control). Units: 0.1°C.

Level (mb)	El Nino (g/kg)	Control (g/kg)	El Nino - Control (g/kg)
1000	18.3	17.2	1.16
850	11.0	8.7	1.28
700	5.6	4.9	0.66
500	2.4	1.9	0.47
400	1.4	0.9	0.33
300.	0.4	0.3	0.11
250	0.2	0.1	0.05
200	0.1	0.1	0.01

Table 1: The time and zonal mean specific humidity at the equator for the two cases.

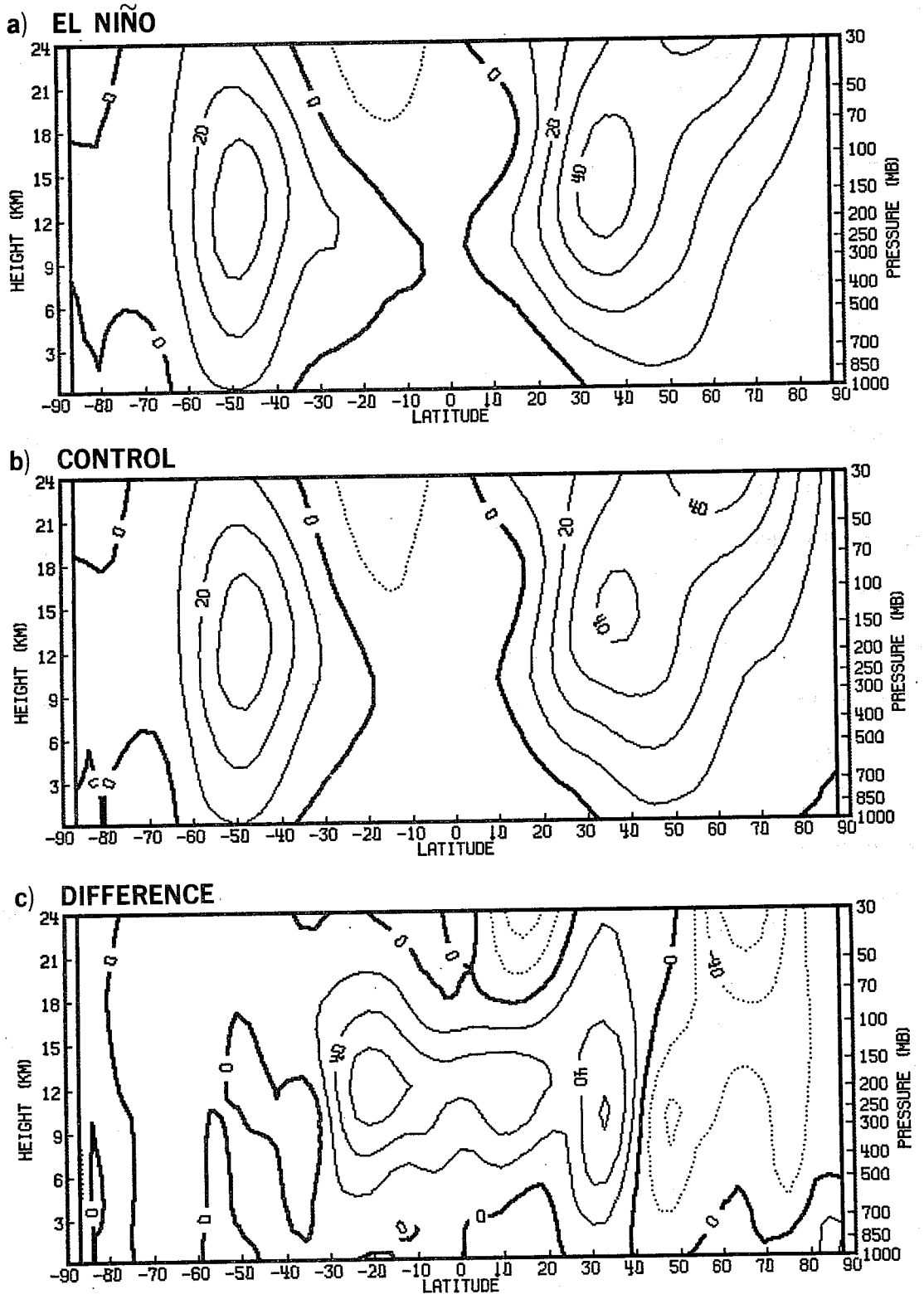

Fig. 4 The zonal mean of the zonal wind for (a) the El Nino case, (b) the Control and (c) the difference (El Nino-Control). Units: top-m/s; middle-m/s; bottom-0.1m/s.

narrower tropical easterlies. This effect contradicts Bjerknes, who suggests that the westerlies should increase in strength rather than extend laterally.

However, in order to assess this mechanism a detailed study of the momentum balance is necessary, but this would exceed the scope of our investigation. It is also not clear to what extent the fact that the model has not reached its equilibrium influences this result.

It is interesting to consider the implications of this finding to model integrations in general. It has been established that in the ECMWF model (as well as in other models) that the subtropical jet is shifted too far towards the poles (Hollingsworth et al., 1980; Cubasch, 1982). This implies that the cause of this poleward shift of the jets might well be a Hadley circulation which is too weak and/or an underestimation of the forcing which drives the Hadley circulation.

The weakening of the westerlies in high latitudes in the northern hemisphere is in accordance with the weakening of the temperature gradients as shown in Fig. 3.

Table 2 shows the tropical maxima of the zonal mean meridional wind in the two cases. The cross-section of the meridional wind difference between the two cases is presented in Fig. 5. These figures show that the near-surface equatorward flow and their upper return flow is intensified in the El Nino case, again similar to the results of long integrations by Cubasch (1985).

Substantial changes occur in the tropics in the vertical velocity component (Fig. 6). In the control case the ascending motion in the tropics is split into two branches, whereas in the El Nino case the vertical motion is more

		El Nino		Control	
		Speed	Lat	Speed	Lat
Southern Hemisphere	Low level	-0.38	20°S	-0.28	26°S
	Upper level	1.66	20°S	1.47	30°S
Northern Hemisphere	Low level	1.55	9°N	1.49	12°N
	Upper level	-3.49	15°N	-3.17	15°N

Table 2: The wind speed (m/s) and the latitude of the centres of the zonal mean meridional wind in the tropics in the two experiments.

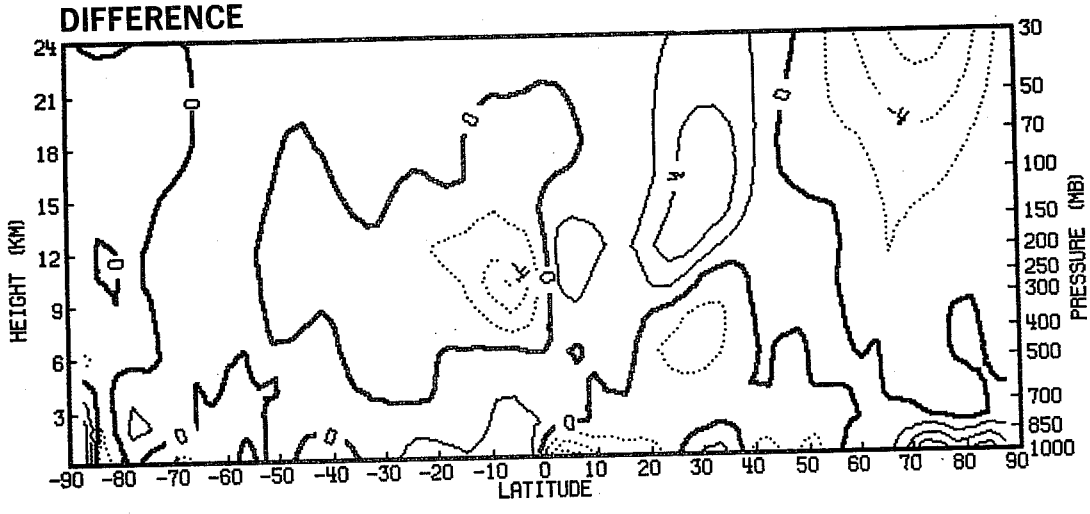

Fig. 5 The difference in the zonal mean meridional wind (El Nino-Control). Units: 0.1m/s.

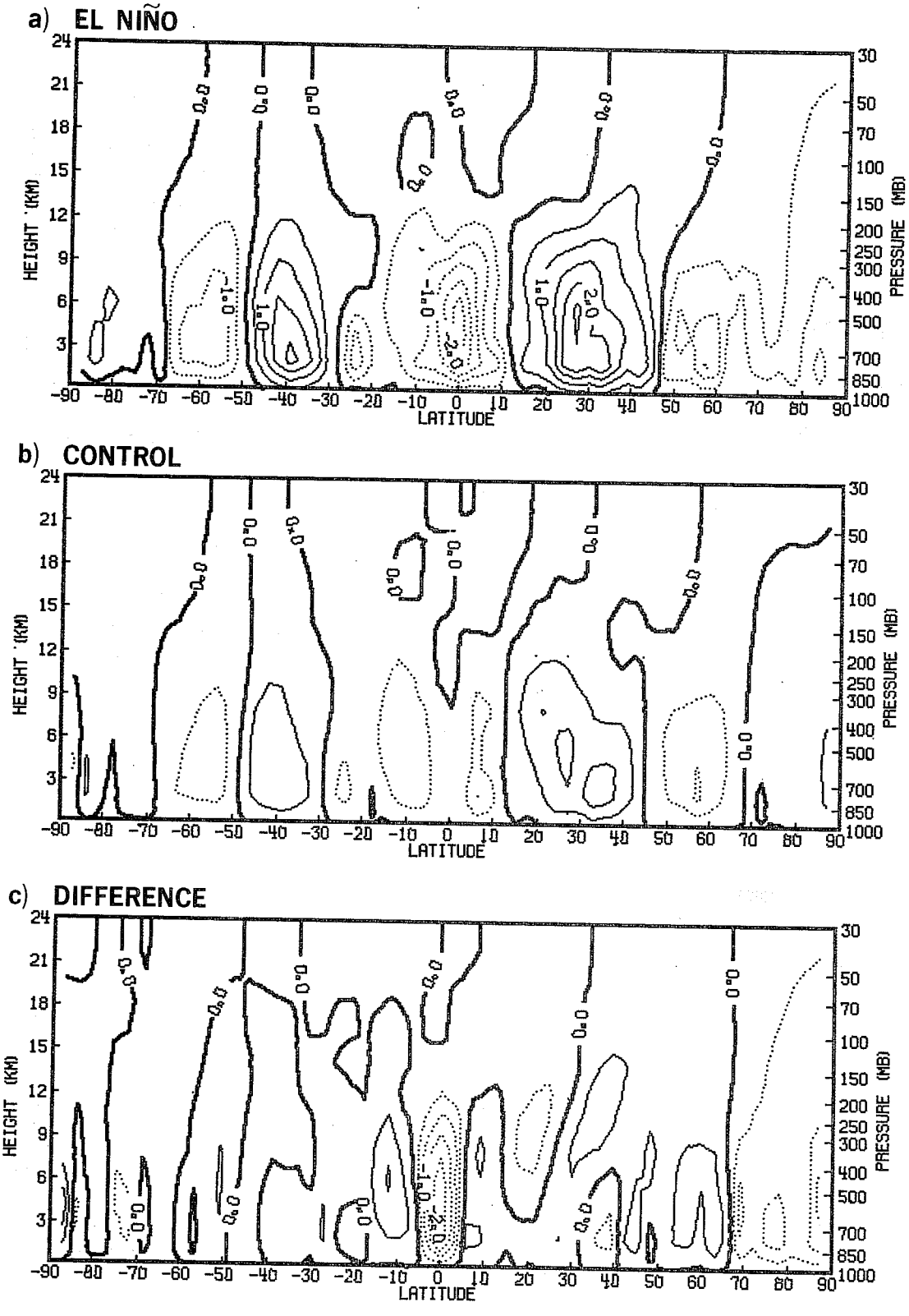

Fig. 6 As Fig. 4, but for the zonal mean vertical wind. Units: 10^{-4} mb/s.

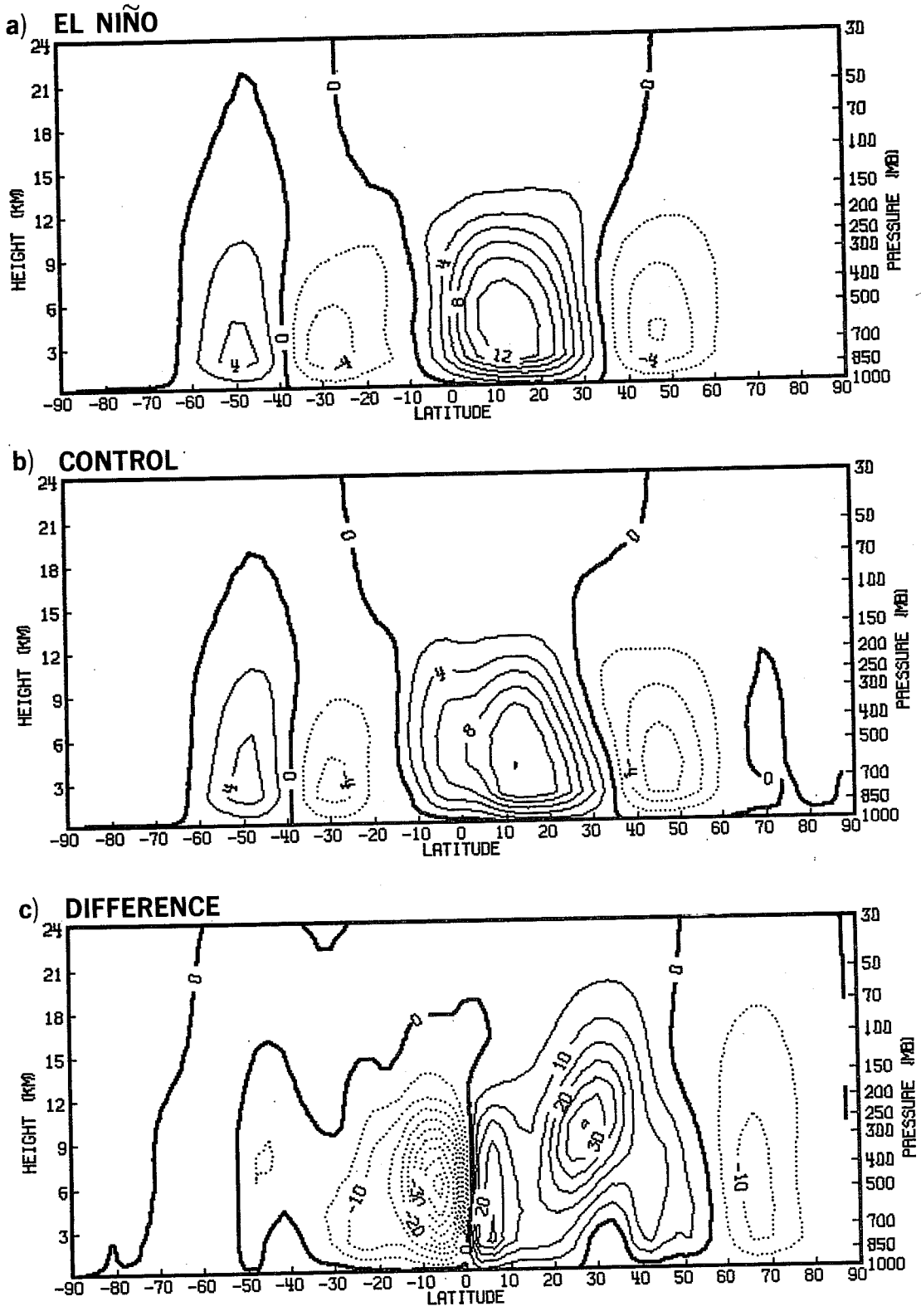

Fig. 7 As Fig. 4, but for the mean meridional circulation
Units: top and middle - 10^7 tons/s; bottom-10^6 tons/s.

		El Nino		Control	
		Int	Lat	Int	Lat
Southern Hemisphere	Ferrel Cell	50.	48°S	51.	48°S
	Hadley Cell	-57.	27°S	-50.	30°S
Northern Hemisphere	Hadley Cell	138.	12°N	123.	13°N
	Ferrel Cell	-65.	46°N	-73.	45°N

Table 3: The intensity (10^6 tons/s) and location of the mean meridional mass flux in the two experiments.

organized with a strong centre of about 3 x 10^{-4} mb/s at 700mb at the equator.

The intensification of the equatorward low-level flow in the tropics and of the ascending motions at the equator lead to an intensification of the Hadley cells as shown in Fig. 7 and Table 3. In particular, the northern Hadley cell is enhanced by 12%. The two Ferrel cells appear to be slightly weakened. The mass flux difference shows clearly an intensification of the toroids (i.e. the direct circulation) over the whole globe except in high latitudes, where an indirect cell can be found in the northern hemisphere; this is caused by the shift of the Ferrel cell rather than by its intensification. The global intensifications of the direct cells implies that the diabatic heating must be the dominant driving factor.

3.2 Transfer properties of the model atmosphere

Fig. 8 presents cross-sections of eddy momentum flux for the El Nino case and the difference in the flux between the two cases, as well as the vertical integrals.

The changes of eddy momentum flux occur mainly in the winter hemisphere, especially in the upper stratosphere. These can be attributed to planetary scale waves. The decrease of momentum flux in the troposphere indicates a less asymmetric wave system, whereas the strong increase of momentum flux in the stratosphere implies a substantial increase of horizontal tilting of planetary scale waves. The vertical integrals of angular momentum flux

$$\int_{p_1}^{p_2} 2\pi a^2 \cos^2\phi \, \overline{uv} \, \frac{dp}{g}$$

with p_1 = 30mb and p_2 = 1000mb does not change much in the two experiments.

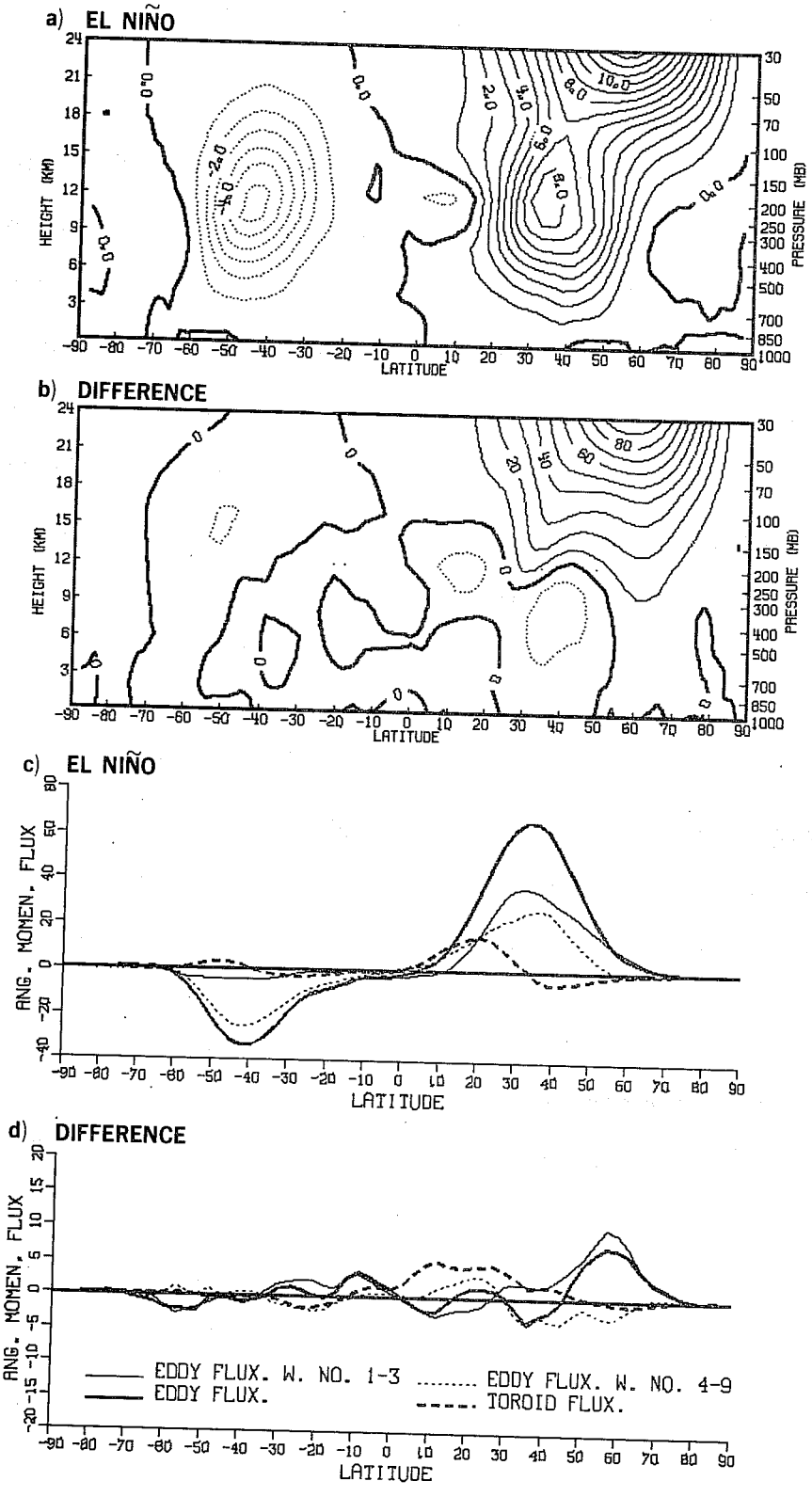

Fig. 8 The zonal mean momentum flux of the eddies for (a) the El Nino case. Units: $10m^2/s^2$ (b) the difference (El Nino-Control). Units: m^2/s^2

Also the vertically integrated momentum fluxes for (c) the El Nino case. Units: Hadley. (d) the difference (El Nino-Control). Units: Hadley.

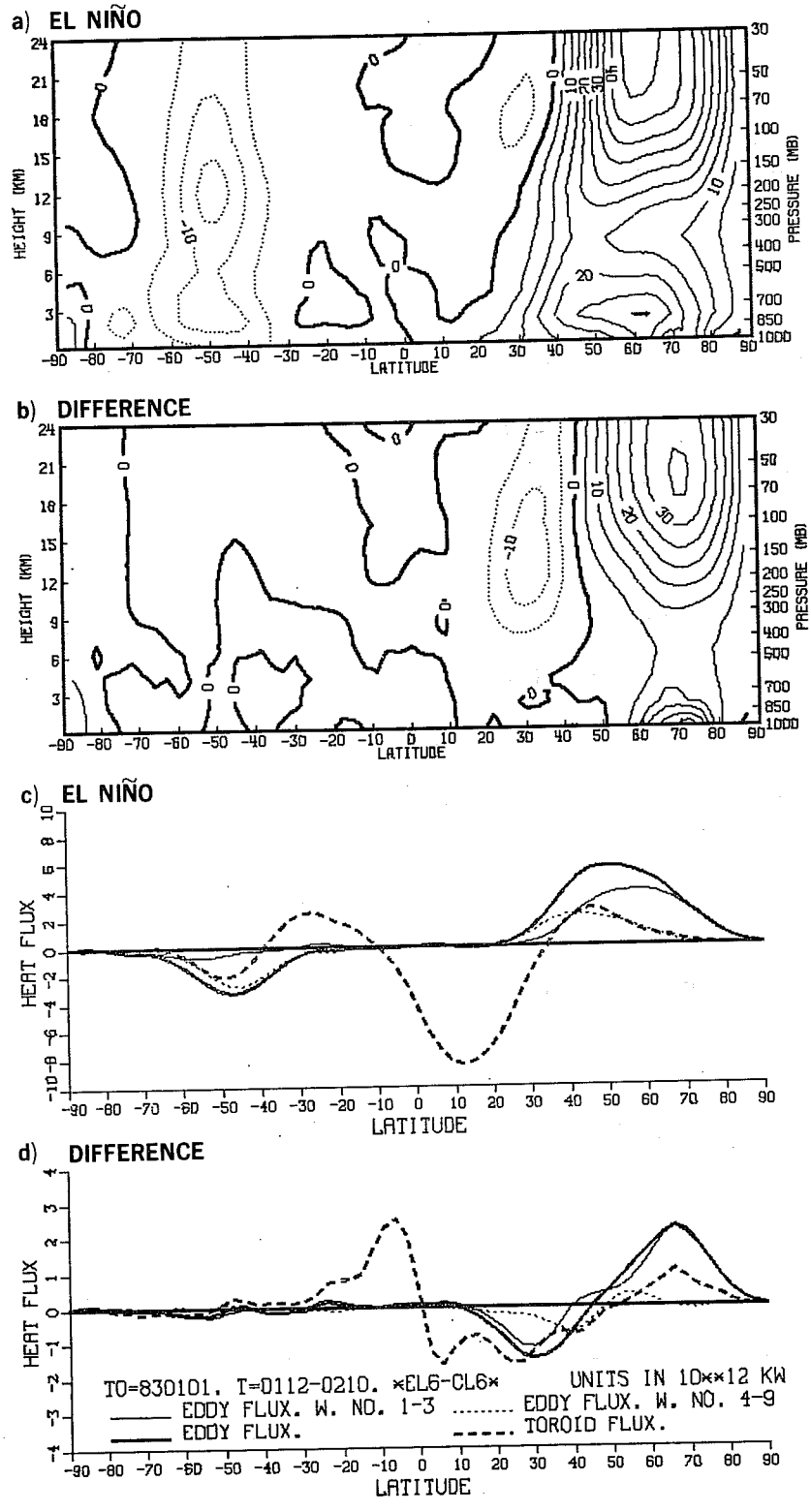

Fig. 9 The zonal mean sensible heat flux of the eddies for (a) the El Nino case. Units: K m/s. (b) the difference (El Nino-Control) Units: K m/s.
Also the vertically integrated momentum fluxes for (c) the El Nino case. Units: 10^{12}kW. (d) the difference (El Nino-Control). Units: 10^{12}kW.

This is similar to results of numerical experiments of mechanical forcing reported by Manabe and Terpstra (1974), and Wu and Tibaldi (1984b). The enhanced toroidal flux in low latitudes results from the intensification of the direct cells, while the enhanced eddy flux must be attributed to the increased horizontal tilting of waves.

Fig. 9 displays the heat flux in a similar fashion as in Fig. 8. The eddy heat flux in the northern stratosphere in the El Nino case reveals the existence of an equatorward heat flux centred in the subtropics of the northern hemisphere, which does not appear in the climate case. It is interesting to notice that its location coincides with the maximum gradient between the additional warming in mid-latitudes and the cooling in low latitudes (see Fig. 3).

The eddy heat flux appears to be shifted further north.

The vertical integral of heat flux

$$\int_{p_1}^{p_2} 2\pi a \cos\phi \, \overline{vT} \, \frac{dp}{g}$$

indicates that the eddies have a more important role in the mid-latitudes in transferring sensible heat polewards, while the toroid plays a major part of transferring heat equatorwards. The poleward shift of the heat flux in high latitudes is reflected in the eddies and toroids, while the equatorwards heat transport in low latitudes can be attributed to the toroidal circulation.

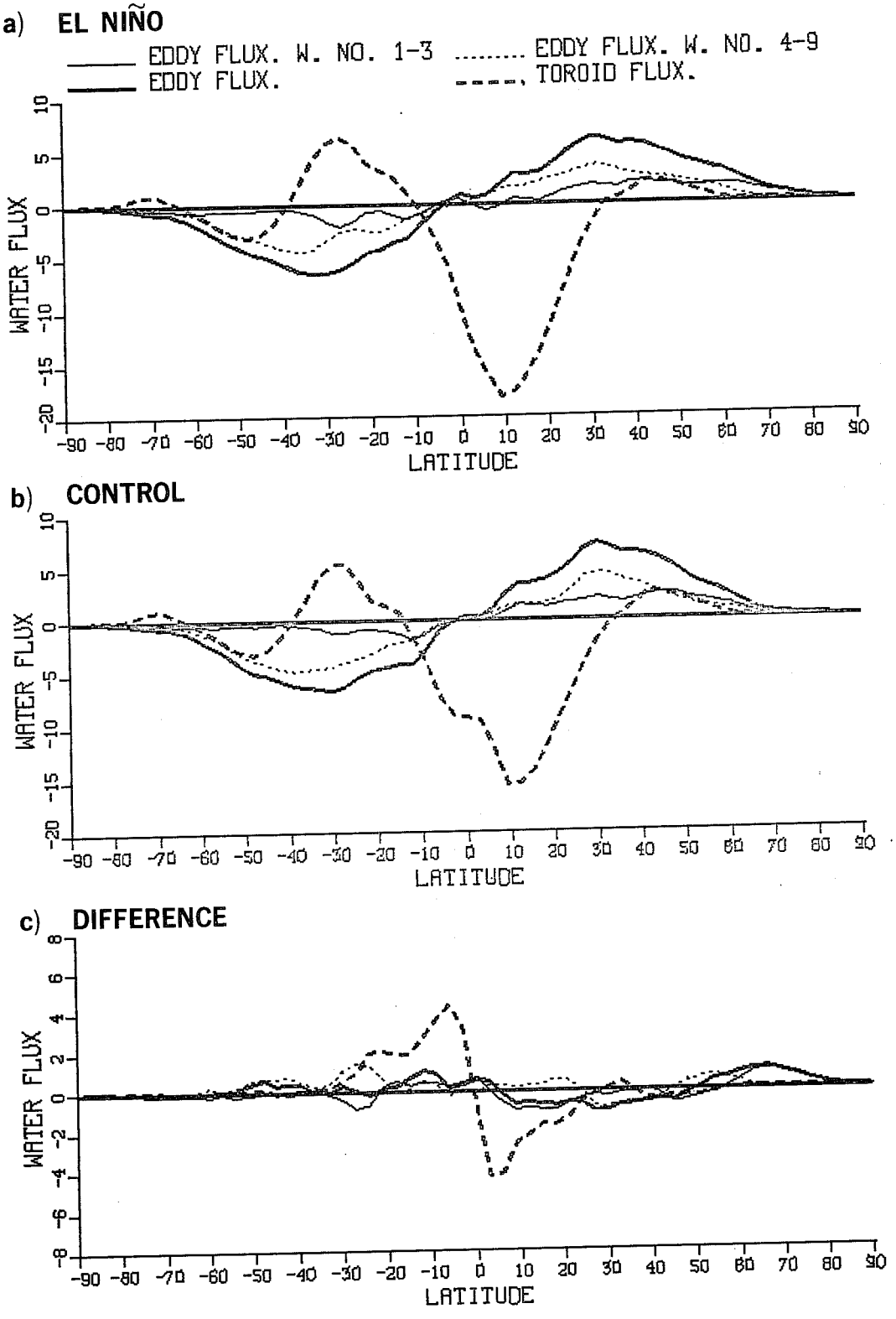

Fig. 10 The zonally and vertically integrated moisture flux for (a) the El Nino case, (b) the control and (c) the difference (El Nino-Control). Units: 10^5 tons/s.

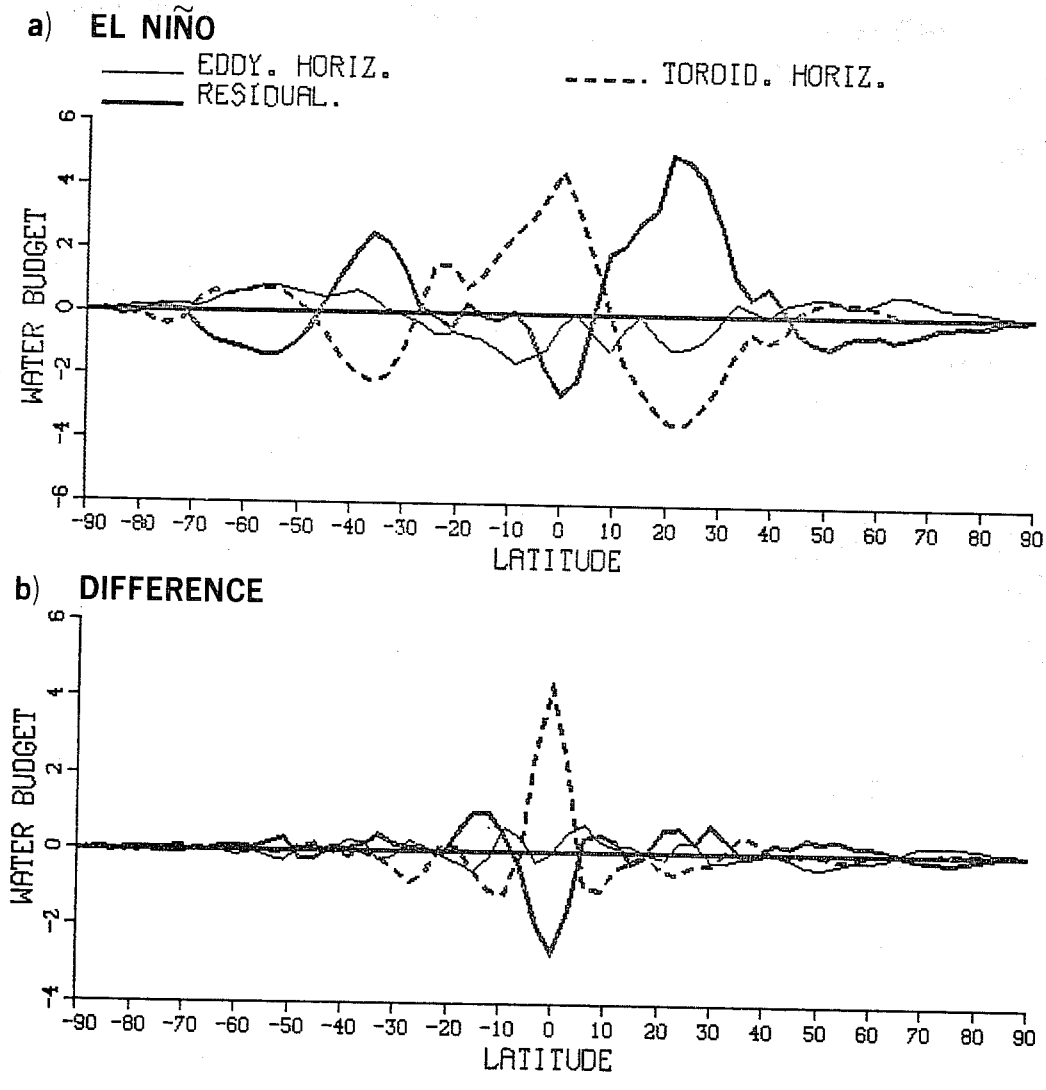

Fig.11 The zonally and vertically integrated moisture budget for (a) the El Nino case and (b) the difference (El Nino-Control). Units 10^5 tons/s.

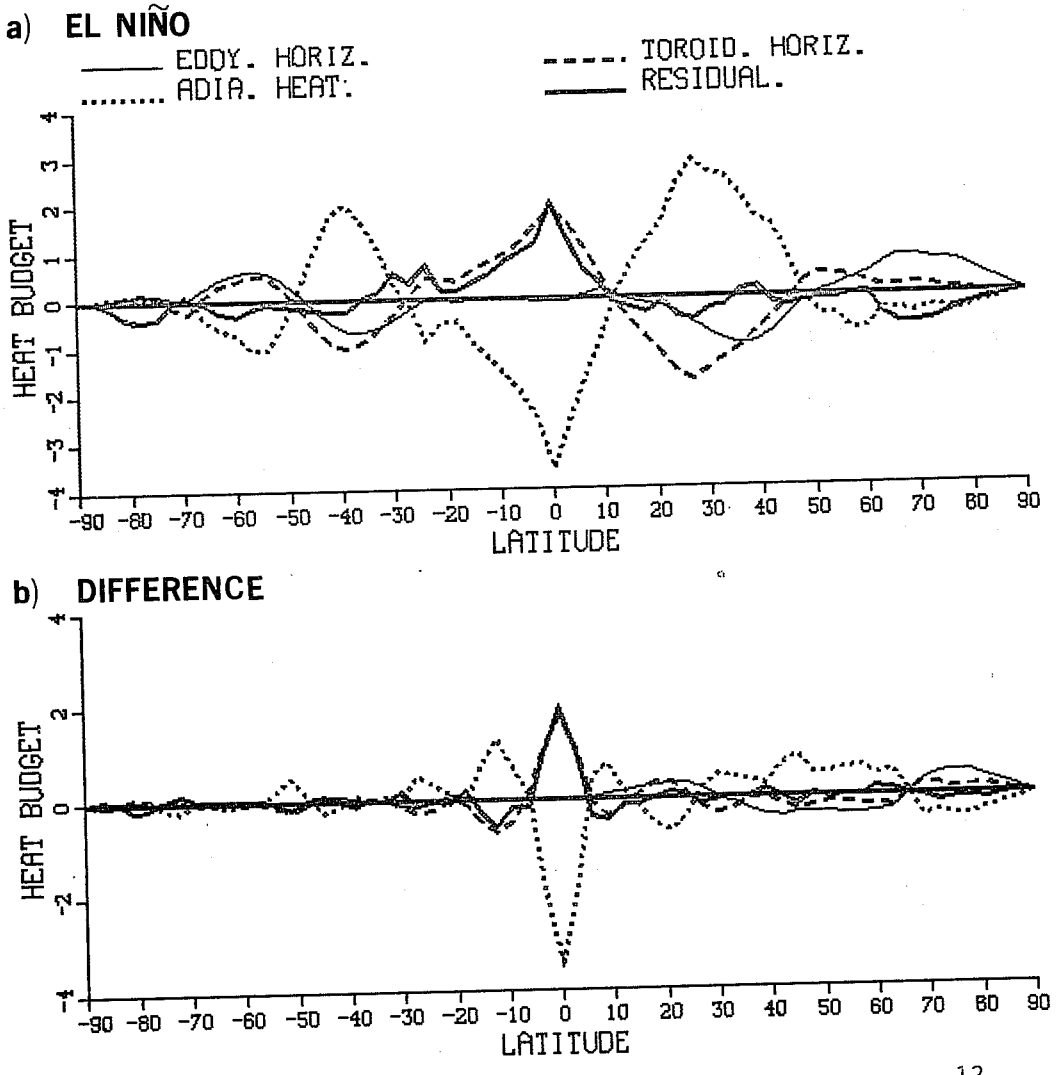

Fig. 12 As Fig. 11 but for the heat budget. Units: 10^{12} kW.

Fig. 10 shows the vertically integrated water flux. The toroidal flux appears to have a similar shape to the observed climatological mean (Newton, 1972). In the El Nino case, due to the intensification of the Hadley cells, much more water is transported towards the equator. The eddy flux is generally polewards in both hemispheres. In low latitudes its changes are relatively small in comparison to the toroidal flux. Even so, it is worthwhile mentioning that the eddy flux is reduced in the El Nino case, and therefore enhances the moisture convergence towards the equator.

3.3 Budgets of moisture and heat

In this section the dominant terms in the budget equations of moisture and heat are investigated. The term "residual" refers to sources or sinks in the corresponding budget equations; for details see Wu and Tibaldi (1984a).

The vertical integrals of the moisture budget is shown in Fig. 11. They indicate that the toroids collect moisture from subtropical areas and transport it towards the tropics. Thus subtropical areas are important water sources whereas the equator is a water sink in both experiments. However, in the El Nino case, this cycle is intensified and results in a maximum of moisture convergence by the toroidal flux, and of moisture sinks in the subtropics.

In the tropics there is a diabatic heat source (Fig. 12). The convergence of eddy heat flux is important in high latitudes, while the toroidal heat flux is dominant in the tropics. The adiabatic cooling resulting from the toroidal circulation balances to a large extent both the diabatic heating and the

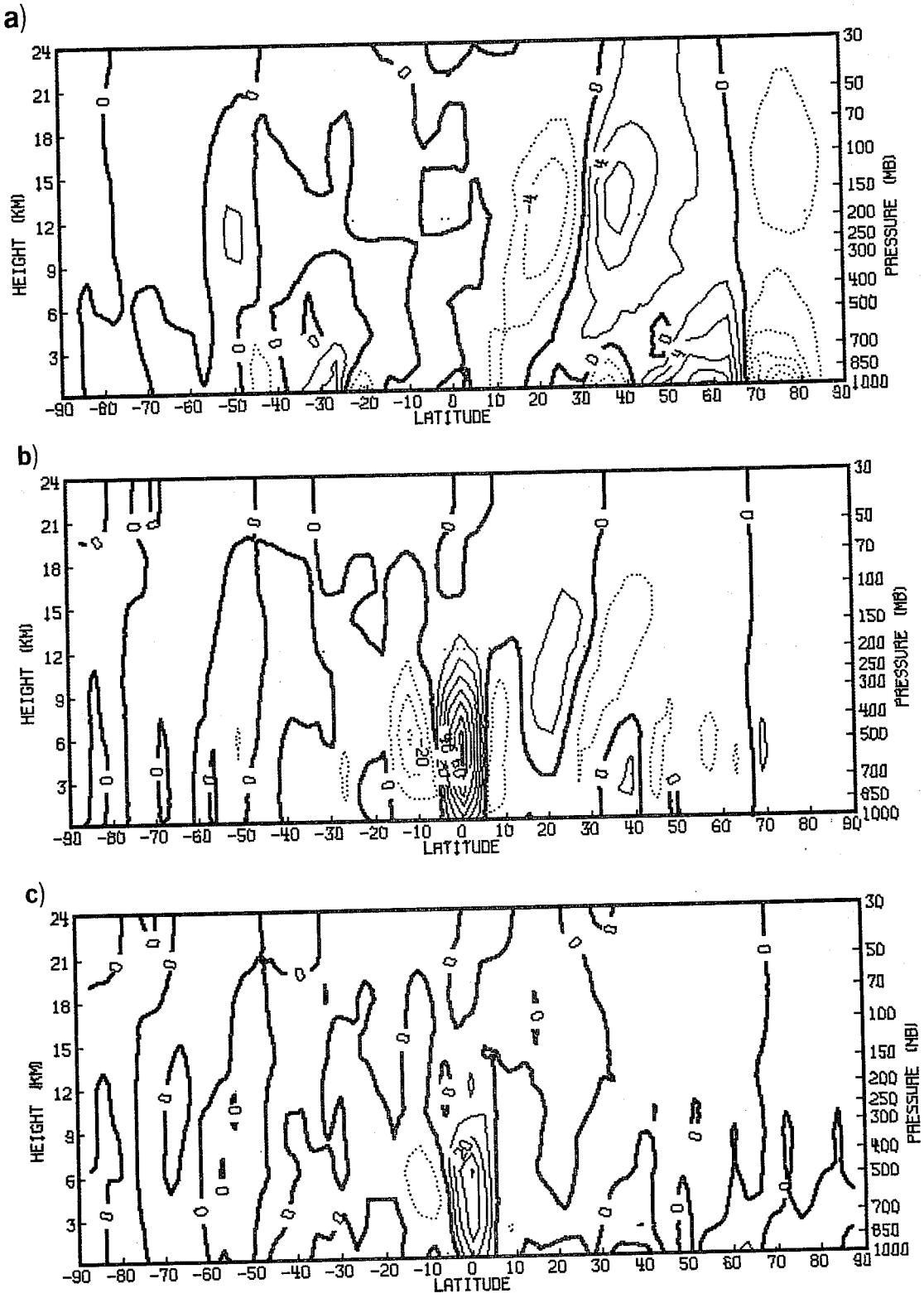

Fig. 13 The difference (El Nino-Control) of the three main terms in the heat budget equation. (a) horizontal divergency of eddy sensible heat flux, (b) adiabatic cooling and (c) heat sources. Units: 10^{10} kW.

convergence of heat flux due to toroids and/or eddies in the tropics. This agrees with the results of Wu and Tibaldi (1984b).

The difference budgets between the two experiments shows an extrema of heating at the equator. To a large extent this heating must come from latent heat release. This, together with the additional convergence of toroidal sensible heat flux is balanced by the adiabatic cooling from the intensified ascent in the Hadley cells.

In Fig. 13 we present the three main terms in the heat budget equation for the difference fields. From these figures we see the following phenomena: in low latitudes the toroids are intensified to balance the additional diabatic heating during an El Nino event. In high latitudes an additional circulation has been generated to counteract the additional poleward fluxes of heat and momentum.

4. CONCLUDING REMARKS

Even though the model atmosphere has not reached an equilibrium state, we see an impact of the equatorial SST anomalies on the simulated circulation. The dynamical and thermodynamical diagnosis allows the following interpretation of the main phenomena.

a) The SST anomaly at the equator triggers a positive feedback between the mean meridional circulation and the tropical diabatic heating: the intensified Hadley cells converge more sensible and latent heat towards the equator. The increased release of latent heat in the tropics then accelerates the direct cells further. The stronger direct cells enhance the moisture convergence further and so on.

b) In the horizontal plane, the stronger Hadley cells gains additional planetary momentum. This results in an equatorward shift of the subtropical jet rather than in an increase of its strength.

c) The increased descent in the subtropical branches of the Hadley cells is compensated by a shift of the eddy heat flux in mid-latitudes.

Acknowledgement

The authors wish to express their thanks to C. Brankovic for making the diagnostic package available.

REFERENCES

Alexander, R.C. and R.L. Mobley, 1974: Monthly average sea surface temperatures and ice pack limits on a 1 degree global grid. Rand report R 1310-ARPA.

Bjerknes, J., 1966: A possible response of the atmospheric Hadley circulation to the equatorial anomalies of the ocean surface temperature. Tellus, 18, 820-829.

Bjerknes, J., 1969: Atmospheric teleconnections from the equatorial Pacific. Mon.Wea.Rev., 87, 163-172.

Cubasch, U., 1981: The performance of the ECMWF model in 50 day integrations. ECMWF Tech. Rep. No. 32.

Cubasch, U., 1982: Sensitivity of the ECMWF model to changes in the resolution. Proceedings to the ECMWF Workshop on Intercomparison of large scale models used for extended range forecasts. ECMWF, Shinfield Park, Reading, UK.

Cubasch, U., 1985: The mean response of the ECMWF global model to the El Nino anomaly in extended range prediction experiments. Submitted to Ocean-Atmosphere.

Greb, M. and B. Nanjokat, 1983: Nordhemisphärischer Kluud bericht zum Februar 1983. Beitrage zur Berliner Wetterkaste des Institutes für Meteorologie der FU Berlin, Berlin, W. Germany.

Hollingsworth, A., A. Arpe, M. Tiedtke, M. Capaldo and H. Savijärvi, 1980: The performance of a medium-range forecast model in winter: Impact of physical parametrisations. Mon.Wea.Rev., 108, 1736-1773.

Kidson, J.W., D.G. Vincent and R.E. Newell, 1969: Observational studies of the general circulation of the tropics: long term mean values. Quart.J.Roy.Met.Soc., 85, 258-287.

Louis, J.-F., (Editor), 1984: The ECMWF forecasting model. ECMWF, Shinfield Park, Reading, U.K.

Manabe, S. and T.B. Terpstra, 1974: The effects of mountains on the general circulation of the atmosphere as identified by numerical experiments. J.Atmos.Sci., 31, 3-42.

Newton, C.W., 1972: Southern hemisphere general circulation in relation to global energy and momentum balance requirements. Meteor. Monogr., 13, 215-246.

Reynolds, R.W., 1984: The 1982/83 El Nino sea surface temperatures. Climate Analysis Centre, NMC, Washington D.C., USA.

Shukla, J., and J.M. Wallace, 1983: Numerical simulation of the atmospheric response to equatorial Pacific SST anomalies. J.Atmos.Sci., 90, 1613-1630.

Wu Guo-xiong and S. Tibaldi, 1984a: The mean meridional circulation and its role in atmospheric motions. ECMWF, Shinfield Park, Reading, U.K.

Wu Guo-xiong and S. Tibaldi, 1984b: The effects of mechanical forcing an the mean meridional circulation of the atmosphere. ECMWF, Shinfield Park, Reading, U.K.